Chimia 55 (2001) 562–569

ISSN 0009–4293

Exploration of Structure-Property Relationships

Jürgen Schreuer*

Abstract: Electrostriction and elasticity provide highly sensitive probes for the exploration of structure-property relationships. With the aid of modern high-resolution capacitive dilatometers reliable linear and quadratic electrostrictive constants can be determined. The unusual thickness dependence of the converse piezoelectric effect in α-quartz and the electrostrictive behavior of the alkali halides are presented as examples. The close correlations between elastic properties and crystal structures are reflected by several heuristic and empirical rules. Resonant ultrasound spectroscopy (RUS) belongs to the most promising methods for the determination of elastic constants in the acoustic frequency regime. The potential of RUS for the simultaneous investigation of elastic and electrostrictive properties including electromechanical coupling effects is discussed.

Keywords: Crystal physics · Elasticity · Electrostriction · Piezoelectricity · Structure-property relationships

1. Introduction

Since the establishment of the first lattice theoretical models about 100 years ago, the interpretation of structure-property relationships ranks among the most important tasks in solid-state sciences. Models possessing high predictive power can help, for instance, to provide structural and physical data of solids under extreme conditions which are not accessible by experiment, and to tailor new materials with special properties. The different modeling approaches either make use of transferable force fields determined by certain adjustable parameters or rely on first principles calculations. While the advantage of empirical models lies in their high computational efficiency, the often poor accuracy and the limited availability of transferable potentials make the use of quantum mechanical methods desirable. Although the basic concepts were developed in the twenties and thirties of the last century, it was the advent of modern computers that eventually made *ab initio* calculations feasible. A detailed overview of computational methods in crystallography and mineralogy has been recently given by Winkler [1].

Besides the fascination for this development one should bear in mind that the interpretation of properties is not exclusively the ability to predict properties from first principles, but rather to reveal the relations between chemical composition, structure and properties of a broad variety of crystalline materials. In this context one has to face the following questions: (i) Is the present amount of available experimental data sufficient for the derivation of general relations and rules? (ii) Which important properties will not be easily accessible by calculations in the near future? (iii) Is there a great difference between a crystal described by computer simulation and a real macroscopic individual? These topics have been controversially discussed on two workshops [2] organized by the Laboratory of Crystallography of the ETH Zürich. In order to illustrate the motivation for our own research in the field of crystal physics, I would like to address these questions briefly.

To date the complete sets of elastic constants of about 2000 crystal species are known. At a first glance this seems to be a remarkable number. In fact it is less than 1% of the crystalline materials with known crystal structure. In the case of higher order effects the situation is even more dramatic. Among the different reasons for the large discrepancy between importance and experimental knowledge of macroscopic physical properties, the lack of high quality crystals of sufficient size is certainly the most important. Added hindrances against a broader investigation of crystal properties are the high technical effort for development and maintenance of the mostly self-made experimental set-ups, and the high expenditure of time on preparation and measurement of samples.

As second order derivatives of thermodynamical potentials the elastic stiffnesses are directly connected with quantities in which the lattice energy per unit volume is involved. The Christoffel determinants combine the elasticity tensor with the propagation velocities of sound waves and related properties such as Debye temperature, thermal conductivity, thermal expansion (Grüneisen relation), melting temperature (Lindemann formula), infrared resonance frequencies and dielectric behavior. Therefore a general qualitative interpretation of elastic properties – in some favorable cases also nearly quantitative – will open access to such other properties. With regard to possible applications, additionally piezoelectric properties and electromechanical coupling effects are of considerable interest. Higher order effects provide access

*Correspondence: Dr. J. Schreuer
Laboratorium für Kristallographie
ETH Zürich
Sonneggstr. 5
CH-8092 Zürich
Tel.: +41 1 632 3752
Fax: +41 1 632 1133
E-Mail: schreuer@kristall.erdw.ethz.ch
http://www.kristall.ethz.ch/LFK

to the anharmonicity of lattice potentials. For small and high symmetry structures calculations from first principles nowadays yield elastic constants which agree to within a few percent with experimental data [3]. However, these calculations are still restricted to the athermal limit. Moreover, the consideration of temperature effects will remain nearly impossible in the foreseeable future.

The answer to the third question is definitely 'Yes'. On the one hand, it is intrinsically impossible to obtain a real crystal without defects (the surface is the worst possible defect). On the other hand, certain electrical and optical properties are known to be strongly influenced by point defects and dislocations. For many properties no systematic study of their dependence on different types of defects has been performed at all. Deviations from the periodic structure are currently not tractable by computational methods. Even with a supreme effort only a negligible, probably non-representative part of a real macroscopic crystal, which consists of about 10^{23} atoms, can be modeled.

Therefore, our work focuses on the improvement and development of dynamic methods for the experimental investigation of electromechanical properties of small samples. Employing these techniques we study the elastic and electrostrictive properties of crystals as a function of external forces and of their real structure.

2. Electrostrictive Effects

The best criterion to test lattice theoretical models is proof of their predictive power. One of the rare examples where a crystal property was predicted without previous experimental knowledge is provided by quadratic electrostriction [4]. Such electromechanical effects represent the second approximation of the mechanical response of matter on an applied electric field. In 1969 Grindlay and Wong [5] proposed a model of the 'elastic dielectric' and first calculated the quadratic electrostriction in some alkali halides of rocksalt structure type. The straightforward calculation encouraged the authors to suggest quadratic electrostriction as a useful probe for the anharmonicity of interionic forces. Unlike for the coefficients of thermal expansion, the relationship between the higher order electrostrictive coefficients and the anharmonicity of the lattice potential is relatively simple since temperature effects can be neglected in first approximation. The interest in quadratic electrostriction is further stimulated by their fundamental relation to some non-linear optical effects such as stimulated Brillouin scattering and quadratic electrooptic effects (Kerr effect).

Table 1. Typical values for longitudinal deformations Δl of a sample with thickness l = 1 mm caused by thermal expansion, linear and quadratic electrostriction, respectively.

Property	Value	Force	Induced change in length
thermal expansion	$\alpha'_{11} = 50 \cdot 10^{-6}K^{-1}$	$\Delta T = 1K$	$\Delta l = 50$ nm
linear electrostriction	$d'_{111} = 2 \cdot 10^{-12}mV^{-1}$	$E = 10^{6}Vm^{-1}$	$\Delta l = 2$ nm
quadratic electrostriction	$d'_{1111} = 5 \cdot 10^{-21}m^2V^{-2}$	$E = 10^{6}Vm^{-1}$	$\Delta l = 0.005$ nm

The mechanical strains ε_{ij} induced by an electric field **E** with components E_k are described phenomenologically by the Taylor series expansion

$$\varepsilon_{ij} = d_{ijk}E_k + d_{ijkl}E_kE_l + ...,$$

where the coefficients d_{ijk}, d_{ijkl} *etc.* denote the corresponding first, second and higher order electrostrictive material properties.

The components d_{ijk}, often referred to as converse piezoelectric constants, form a polar third-rank tensor. Therefore, linear electrostriction can only occur in crystals with a non-centrosymmetric point symmetry group (PSG), with the exception of PSG 43. Linear electrostrictive effects are in the order of $10^{-12}mV^{-1}$ (Table 1) and can be easily measured employing optical or electromechanical dilatometers [6]. Due to the important technical applications of piezoelectric materials (piezoelectric actuators, sensors, oscillators, switches, frequency filters *etc.*) most of the recent work is devoted to the search for new non-centrosymmetric crystal species possessing large polar properties.

In contrast to linear electrostriction, quadratic effects, represented by a polar 4th rank tensor $\{d_{ijkl}\}$, exist in all crystals and even in amorphous materials. However, in non-ferroelectric compounds these effects are rather small. Particularly, the mechanical response of a centrosymmetric crystal on an applied electric field is often barely above the lower limit of detectable strains (Table 1). It is therefore not surprising that the early experimental results for the quadratic electrostriction in alkali halides are contradictory, *i.e.* the tensor components deviate significantly in magnitude and in sign. For example, the literature values of the component d_{1111} of sodium chloride vary between –6.7 and $+34 \cdot 10^{-21}m^2V^{-2}$. Due to the lack of reliable experimental data the interpretation of quadratic electrostriction has stagnated in the last decades. Just recently two research groups, one in the Netherlands [7] and the second in Germany/Switzerland [8], studied the sources of several disturbing effects and developed apparative tools which allow for the successful investigation of quadratic electrostrictive properties.

2.1. *Experimental Approach: High-resolution Capacitive Dilatometer*

Among the different approaches to the determination of quadratic electrostrictive constants ([8] and references therein) the direct strain measurements employing dilatometers based on the frequency-modulation technique are the most promising.

The heart of our capacitive dilatometer [8] (Fig. 1) consists of an oscillator with basic frequency in the range between 60 and 110 MHz. The two electrodes of the frequency-controlling capacitor are supported by transducer rods which are connected with the sample and with a reference crystal, respectively. Thus, a periodic longitudinal deformation of one of the crystals leads to a modulation of the high-frequency signal of the oscillator. The modulation is electronically transformed in a voltage signal that is finally filtered by means of a LockIn amplifier. For small deformations ($\Delta l \leq 10$ nm) the linear relationship $\Delta l = S \cdot A$ between LockIn-amplitude A and deformation Δl holds in sufficient approximation. The factor S can be determined by applying a low voltage ac-signal, $U_{rc} \approx 10$ V, to the reference crystal (for example an X-cut α-quartz specimen) with the effective converse piezoelectric effect d'^{rc}_{111}. The change of length of the sample is now obtained by

$$\Delta l_s = S \cdot A_s = \Delta l_{rc} \frac{A_s}{A_{rc}} = d'^{rc}_{111} U_{rc} \frac{A_s}{A_{rc}}$$

Quantities with subscripts *s* and *rc* are related to the sample and to the reference crystal, respectively. The sign of the elec-

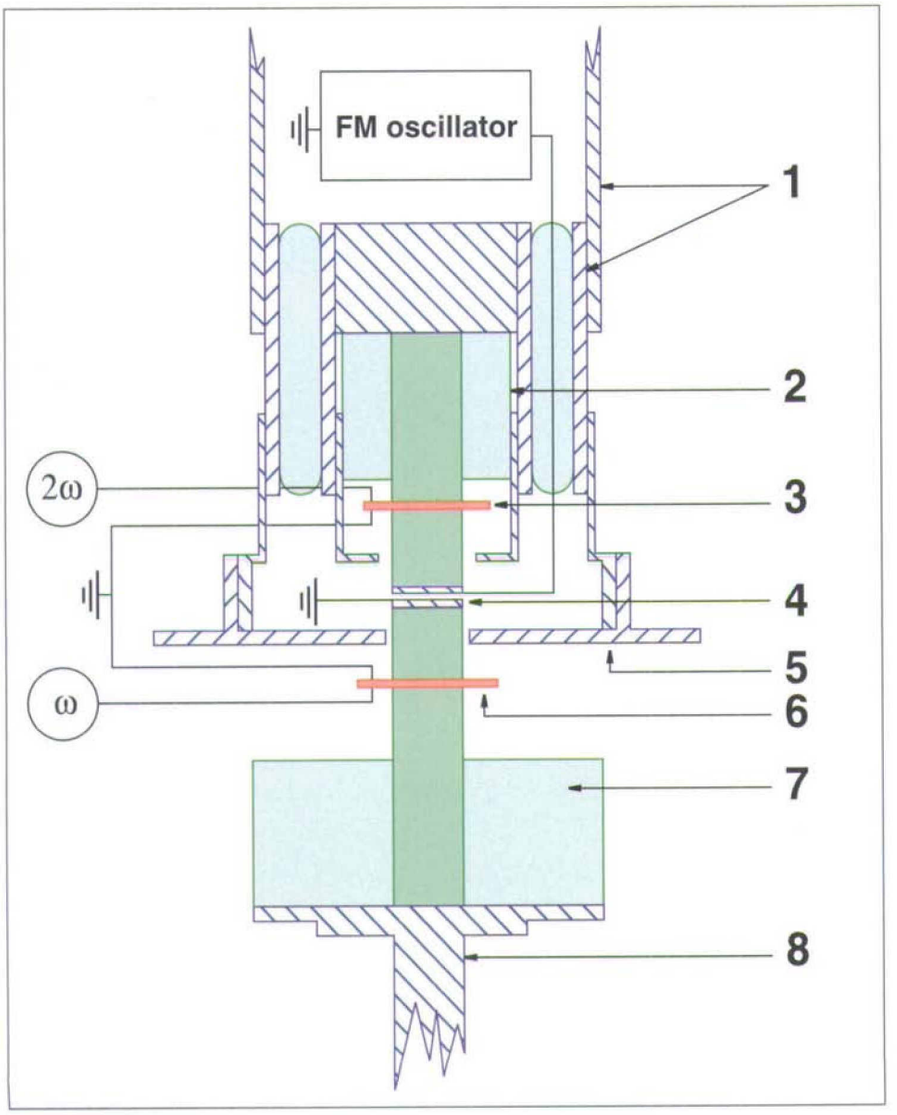

Fig. 1. Sketch of our capacitive dilatometer. 1: electrically shielded oscillator chamber, 2: reference crystal holder, 3: reference crystal, 4: plate capacitor, 5: electrical shielding, 6: sample, 7: sample holder, 8: adjustable support.

trostrictive deformation of the sample can be derived from the phase difference $\Delta\phi = \phi_s - \phi_{rc}$ of the LockIn signals provided that the polarity of the reference crystal is known.

In order to achieve high resolution of about $\Delta l \approx 2 \cdot 10^{-13}$ m thorough measures, as for example good electrical and thermal shielding and excellent vibration isolation, have to be taken to minimize external disturbances. The most critical source of errors are Coulomb-interactions between certain parts of the dilatometer. Particularly, the high-voltage of up to 3 kV required for the investigation of very small quadratic effects leads to strong electromechanical vibrations which superimpose the strain signal caused by the electrostrictive effect of the sample. It is practically impossible to avoid electromechanical resonances, because they depend on shape, dimension and position of the conducting wires. Fortunately, in most cases large intervals without such spurious effects can be tracked down by frequency dependent measurements.

2.2. *Example: Quadratic Electrostriction in Alkali Halides*

Currently, the quadratic electrostrictive coefficients of alkali halides determined with the aid of the new capacitive dilatometer are likely to be regarded as the best available. Earlier experimental data, the spread of which was interpreted by a strong dependence of quadratic electrostriction on impurities and defects [9], should be considered with some reservation. It cannot be excluded that these data suffer from spurious effects as outlined in the previous section.

According to the results obtained by Schreuer and Haussühl [8] on eight alkali halides, the longitudinal component d_{1111} varies between $2 \cdot 10^{-21} m^2V^{-2}$ and $6 \cdot 10^{-21} m^2V^{-2}$, whereas the transversal component d_{1122} always exhibits a negative sign and d_{1212} is one order of magnitude smaller than d_{1111}. The volume-striction $\partial^2 \ln V/(\partial E)^2 = d_{1111} + 2d_{1122}$, a scalar invariant in PSG $m3m$, is positive in all investigated alkali halides and increases with decreasing elastic stiffness. The close correlation between volume-striction and the quantity $\alpha/K = \gamma C_V/3V$ (α linear coefficient of thermal expansion, K compressibility, V molar volume, C_V specific heat capacity at constant strain, γ Grüneisen parameter) shows the anharmonic nature of quadratic electrostriction.

The longitudinal effect $d'_{1111} = u_{1i}u_{1j}u_{1k}u_{1l}d_{ijkl}$ (u_{1i} direction cosine) possesses a strong anisotropy with distinct maxima and minima along ⟨100⟩ and ⟨111⟩, respectively (Fig. 2). At first glance the coincidence of the maxima of d'_{1111} and of the longitudinal elastic stiffness in most alkali halides is surprising. The different behavior of lithium fluoride (Fig. 2), however, indicates that the origin of the electrostrictive anisotropy is different from the origin of the elastic anisotropy. The relative sizes of the cations and anions dictate the directions with close contacts between neighboring ions. Correspondingly, the maxima of the longitudinal elastic stiffness appear in lithium halides along ⟨111⟩ whereas in other alkali halides the maxima are observed in ⟨100⟩ directions. In contrast to the elastic behavior the anisotropy of the quadratic electrostriction is nearly independent of the radius ratio. The dominant contributions to the macroscopic electrostriction stem from the polarizability of the ions and from dispersive interactions between opposite charged ions. This picture is confirmed by lattice energy calculations based on empirical force fields [5][10]. Sufficient agreement between theory and experiment is only achieved by model calculations which adequately take into account short-range interactions.

Although it is not yet a routine examination, our capacitive dilatometer as well as the sophisticated, but slightly less accurate double-beam Michelson-interferometer recently constructed by Sterkenburg *et al.* [7] allow for the determination of reliable quadratic electrostrictive coefficients.

It is expected that a larger amount of experimental data will become available soon and thus will give new impetus to the study of quadratic electro-striction in centrosymmetric crystals.

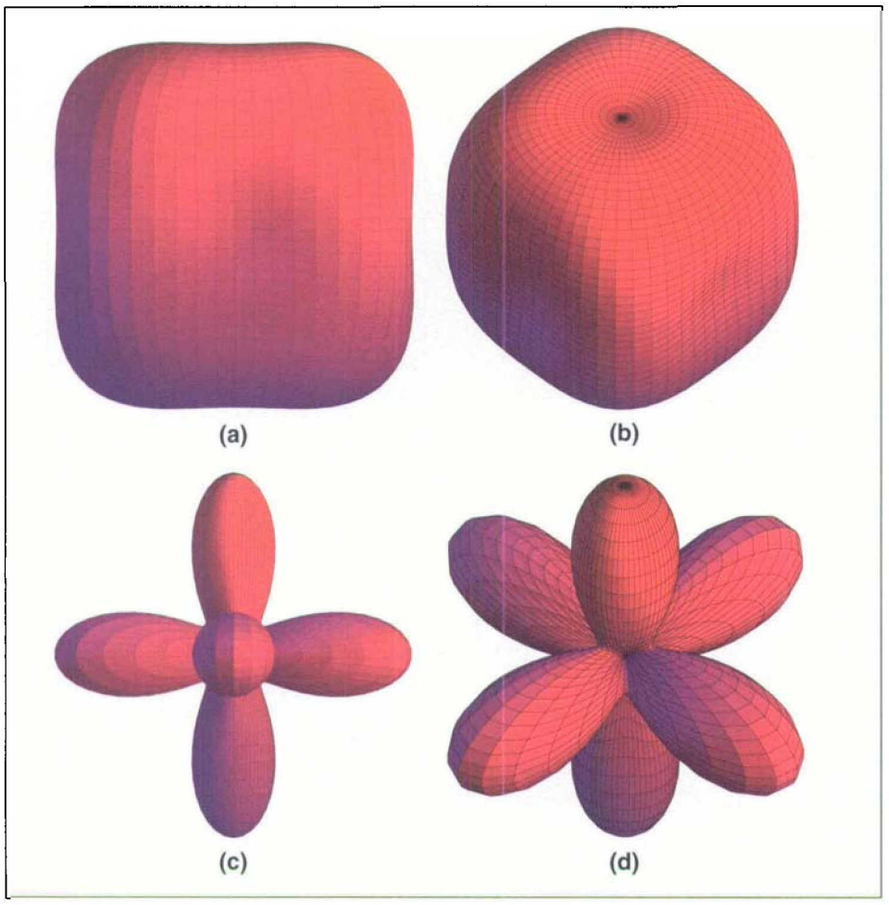

Fig. 2. Representation surfaces of longitudinal elastic stiffness $c'_{1111} = u_{1i}u_{1j}u_{1k}u_{1l}u_{ijkl}$ (u_{1i} direction cosine, $i = 1,2,3$) and of the longitudinal effect $d'_{1111} = u_{1i}u_{1j}u_{1k}u_{1l}d'_{ijkl}$ of quadratic electrostriction in LiF. (a),(b): surface of c'_{1111} viewed along [100] and [111], respectively. (c),(d): surface of d'_{1111} viewed along [100] and [111].

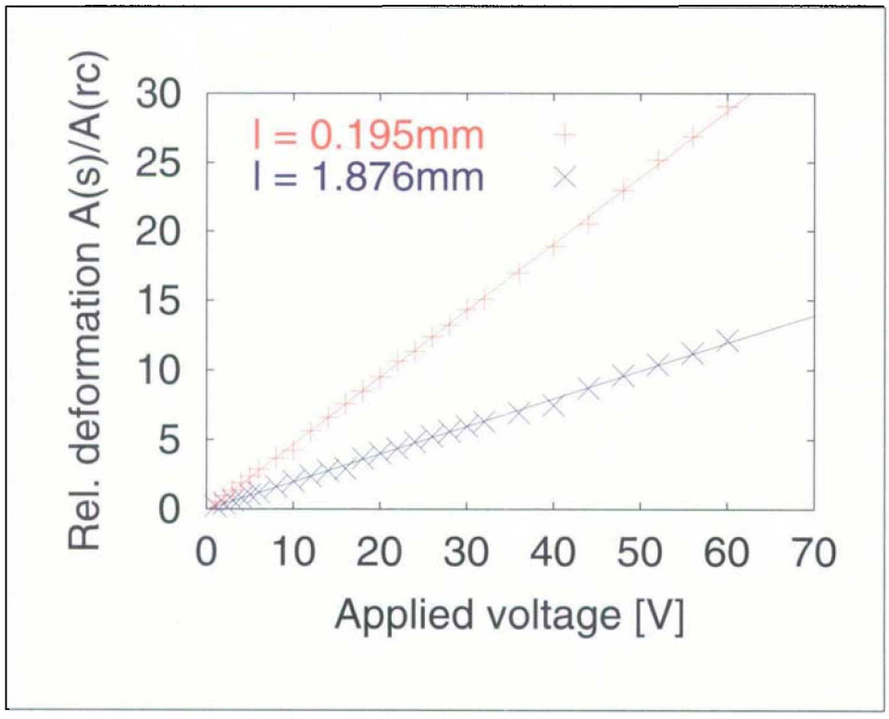

Fig. 3. Relative deformation $\Delta l \sim A_s / A_{rc}$ of two synthetic X-cut α-quartz plates with different thicknesses but equal diameters of about 20 mm as a function of the applied voltage. Reference crystal is a disk-like specimen of X-cut α-quartz with diameter of 20 mm and thickness of 1.872 mm.

2.3. *Thickness Dependence of Converse Piezoelectric Effects*

While testing the high-resolution capacitive dilatometer an unexpected thickness dependence of the longitudinal converse piezoelectric effect was discovered along the polar directions of certain piezoelectric crystals.

The well reproducible thickness effect (Fig. 3) was first observed on thin plates of α-quartz (X-cuts of synthetic and natural crystals with diameters and thicknesses in the ranges 12–40mm and 0.08–13mm, respectively). For $l > 0.5$mm d_{111} increases in proportion to the reciprocal thickness $1/l$ of the specimens. With thinner plates d_{111} gradually reaches a constant value. Crystals of $LiNbO_3$, $NaBrO_3$, $Li_2SO_4{\cdot}H_2O$ and benzil show a similar behavior whereas in $Cs_2S_2O_6$ no influence of the sample thickness on d_{333} is observed. The electrostrictive effect along the six-fold axis in lithium iodate even decreases rapidly with decreasing thickness. Due to the specific behavior of the different crystal species, systematic errors originating from the experimental set-up cannot account for the strange thickness dependence. Further disturbances from electrode effects, excitation of vibrational modes of the samples, boundary conditions and sample mounting have been excluded by experiments.

A simple sandwich model, which is based on the assumption that the electrostrictive properties of the surface zone differ from those of the bulk material, allows for a qualitative interpretation of the observed thickness effects. In the case of quartz the model yields a thickness of about 100–150 μm for the surface zone. The electrostrictive effect $d_{111}^{surface} = 8.5 \cdot 10^{-12}$mV^{-1}is about a factor 3.7 enlarged compared to the value d_{111}^{bulk} of the bulk crystal ($l \rightarrow \infty$). The reason for the variation of electrostrictive properties in sur-

face zones is not yet clear. It is probable that defects which are induced by the preparation procedure play an important role. Further investigations are in progress.

The most surprising aspect of the thickness effect is not the existence of a surface layer possessing different properties, but its extension. A cube with edge lengths of 0.5 mm, 1 mm and 5 mm and surface zones of about 100 μm thickness consists of 78%, 49% and 12% surface zone, respectively. With regard to the ongoing miniaturization of experimental set-ups careful investigations of potential surface zones and their influence on the experimental determination of various physical properties are essential.

3. Elastic Properties of Crystals

Elasticity provides one of the most useful probes for the exploration of structure-property relationships. As spring constants elastic stiffnesses are directly related to the three-dimensional network of interatomic interactions in the crystal and, consequently, to many other of its thermodynamical properties. Hence, elastic constants permit subtle tests of the reliability of atomistic model calculations. Further, elastic constants are highly sensitive to structural instabilities connected with phase transitions. Characteristic anomalies of the elastic behavior allow not only the detection of phase transitions but offer valuable hints on the driving mechanisms [11].

In the linear approximation of Hooke's law the components σ_{ij} of the mechanical stress tensor and the components ε_{ij} of the strain tensor are related by $\sigma_{ij} = c_{ijkl}\varepsilon_{kl}$ where $\{c_{ijkl}\}$ is the elasticity tensor [12]. In the case of electrostrictive crystals Hooke's law must be completed by additional terms which take into account electro-mechanical coupling effects. For small deviations from equilibrium the mechanical and electrical variables of the corresponding thermodynamic potential are related by

$$\sigma_{ij} = c^E_{ijkl}\varepsilon_{kl} - e_{kij}E_k = c^E_{ijkl}\frac{\partial \xi_k}{\partial x_l} + e_{kij}\frac{\partial \phi}{\partial x_k}$$

$$D_i = e_{ikl}\varepsilon_{kl} + \epsilon^S_{ij}E_j = e_{ikl}\frac{\partial \xi_k}{\partial x_l} - \epsilon^S_{ij}\frac{\partial \phi}{\partial x_j}$$

where **E** is the electric field vector and **D** the electric flux density. ξ_k denote the components of the displacement vector, ϕ is the electric potential and $\{\epsilon_{ij}\}$ represents the tensor of the dielectric constants. e_{ijk} are the components of the piezoelectric stress tensor which are related to the coefficients d_{ijk} of the piezoelectric tensor according to $e_{mij} = d_{mkl}c^E_{ijkl}$. Superscripts S and E indicate adiabatic conditions and constant electric field, respectively.

Due to their symmetry properties, the elastic stiffnesses c_{ijkl} are usually written in an abbreviated form employing Voigt's notation, *i.e.* the index pairs ij and kl are replaced by simple indices according to $ij \rightarrow i$ for $i = j$ and $ij \rightarrow 9\text{-}i\text{-}j$ for $i \neq j$. Four types of elastic constants c_{ij} can be distinguished:

c_{11}, c_{22}, c_{33}	longitudinal elastic stiffnesses,
c_{12}, c_{13}, c_{23}	transverse interaction coefficients,
c_{44}, c_{55}, c_{66}	elastic shear stiffnesses,
c_{14}, c_{15}, c_{16}, *etc.*	coupling coefficients.

The number of independent elastic constants of a crystal depends on its point symmetry group. For example, 21 constants c_{ij} have to be determined in order to describe the elastic behavior of a triclinic crystal whereas in cubic crystals the knowledge of three constants (*e.g.* c_{11}, c_{12}, c_{44}) is sufficient. Details about the symmetry reduction of property tensors can be found in many text books dealing with crystal physics and applications of group theory [12–14].

3.1. *Empirical Rules*

For new compounds simple heuristic and empirical rules allow quick estimation of the order of magnitude of certain physical properties (*e.g.* dielectric behavior, refractive indices, certain non-linear optical properties and mean elastic stiffness). These rules are based on the assumption that the constituents of the crystal yield quasi-persistent additive contributions to the various physical properties. Once the crystal structure is known, one can further deduce a qualitative picture of the anisotropy of the properties.

Haussühl [15] discovered that the quantity $S = C \cdot M_V$, defined as the product of the mean value of the principal elastic constants $C = (c_{11} + c_{22} + c_{33} + c_{12} + c_{13} + c_{23} + c_{44} + c_{55} + c_{66})/9$ and the molecular volume M_V, opens the possibility to estimate the mean elastic stiffness of ionic crystals provided that chemical composition and density are known. The S-value varies only slightly within isotypic crystals and chemically related compounds. Furthermore, in ionic crystals the S-value can be decomposed in additive contributions $S(X_i)$ of the constituents X_i of the compound X according to $S(X) = \sum S(X_i)$. The quasi-additivity of the S-values holds within 10% for a large variety of compounds, including spinels, perovskites, garnets and feldspars. Even the influence of water of crystallization can be separated. On the other hand deviations from the rule yield hints on anomalous bonding contributions.

One approach to the qualitative interpretation of the anisotropy of the longitudinal elastic stiffness $c'_{1111} = u_{1i}u_{1j}u_{1k}u_{1l}c_{ijkl}$ is provided by the system of principal bond chains (PBC-vectors according to Hartman and Perdok [16]). Often the maximum of c'_{1111} corresponds with a minimum of the longitudinal thermal expansion $a'_{ij} = u_{1i}u_{1j}\alpha_{ij}$ and both usually occur along the direction of the strongest PBC-vectors (Fig. 4). Instructive examples can be found among the phthalates [18], oxalates [19] and tetroxalates [20]. However, the description of the bonding system in terms of PBC-vectors is not fully compatible with the interpretation of the elastic stiffnesses as spring constants, because it neglects the spatial arrangement of the bonds within a periodic bond chain. The alkali feldspar sanidine, $KAlSi_3O_8$, represents a prominent exception from the rule. Due to the zigzag-like character of the strongest bond chains running parallel to the a_1-axis a longitudinal deformation along [100] is mainly caused by small changes of the O–Si–O bond angles instead by compression or dilatation of the rather stiff Si–O bonds. Consequently, in sanidine the maximum of c'_{1111} is observed along [010], *i.e.* it is located in the plane perpendicular to the main bond chains.

A hint on the nature of the bonding interactions in crystals can be derived from the deviations from Cauchy relations [21] represented by the second rank tensor invariant $\{g_{mn}\}$ with the components $g_{mn} = \hat{e}_{mik}\hat{e}_{njl}c_{ijkl}/2$, where $\hat{e}_{ijk}$ denote the components of the Levi-Civitá symbol. In metallic and ionic crystals, particularly in those built up from aspheric ions and constituents with large polarisability, the transverse interaction coefficients dominate considerably over the corresponding shear stiffnesses resulting in positive deviations from Cauchy relations. Strong covalent or other bonds with preferential directions cause opposite effects. Extreme examples are gold and diamond with $g_{11} \approx +12 \cdot 10^{10}\text{Nm}^{-2}$ and $g_{11} \approx -24 \cdot 10^{10}\text{Nm}^{-2}$, respectively. Crystals possessing a layer-like structure such as gypsum and micas show often a distinct minimum of the deviations from Cauchy relations along the direction perpendicular to the plane of the layers indicating covalent bonding contributions

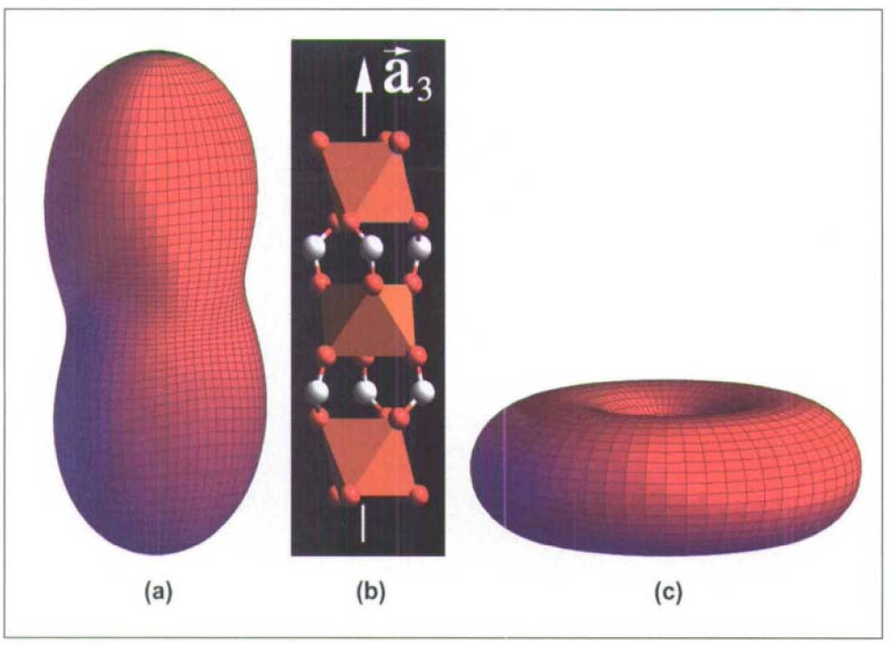

Fig. 4. Correlation between longitudinal elastic stiffness (a), longitudinal effect of thermal expansion (c) and crystal structure (b) of trigonal $((CH_3)_3NCH_2COO)_3{\cdot}2MnCl_2$ [17].

within and weaker Coulomb or van-der-Waals interactions between the layers.

A more quantitative interpretation of elastic behavior can be obtained from lattice energy calculations [1]. Within the framework of thermodynamical potentials elastic constants are defined as second order derivatives of potential functions, *e.g.*

$$c_{ijkl} = \frac{\partial^2 U}{\partial \varepsilon_{ij} \partial \varepsilon_{kl}}$$

Here $U = U(\{\varepsilon_{ij}\},\mathbf{D},S)$ is the free energy, and ε_{ij}, $\mathbf{D}$ and S are the components of strain tensor, the electric flux density and entropy, respectively.

3.2. *Experimental Determination of Elastic Constants*

Many different techniques covering broad frequency-, temperature- and pressure-ranges are available for the experimental investigation of elastic properties [22]:

- Static methods including stretching, bending and torsion experiments.
- Dynamic methods such as periodic stretching, bending and torsion experiments at frequencies below the first mechanical resonance frequency of the sample.
- Ultrasonic methods based on excitation of ultrasonic waves in the sample, *e.g.* normal and improved Schaefer-Bergmann method, pulse-echo techniques, acoustic resonance methods.
- Scattering methods: scattering of photons or neutrons on thermal phonons, *e.g.* Brillouin spectroscopy (scattering of light on acoustic phonons), Raman spectroscopy (light scattering on optical phonons), thermal diffuse X-ray scattering (Compton scattering of X-ray photons), inelastic neutron scattering (phonon spectroscopy).

Other techniques such as the investigation of surface acoustic waves or the application of atomic force microscopy are still in an early stage of development. The potential of laser-induced phonon spectroscopy, LIPS [23], and ultrasonic interferometry in the GHz frequency regime [24] for use with diamond-anvil cells under high pressures is currently explored. Other methods even allow for imaging of phonon propagation in crystals [25].

The most accurate determination of elastic constants in the important acoustic frequency regime is facilitated by ultrasonic techniques. Conventional ultrasonic methods actually determine the velocities of ultrasonic plane-waves injected into the sample. The velocities are derived either from the traveling time of short ultrasonic pulses (pulse-echo techniques) or from resonance frequencies of thick plane-parallel plates (improved Schaefer-Bergmann method, impedance method). Although these techniques are highly sophisticated, their application is limited by a number of problems including transducer ringing, transducer-sample coupling, beam diffraction, the sample size, and the necessity of measuring samples with different orientations in order to estimate all independent elastic constants.

3.3. *Resonant Ultrasound Spectroscopy*

In the last three decades a very powerful alternative experimental approach has become available due to significant advances in computer technology: resonant ultrasound spectroscopy (RUS). Here the elastic constants are derived from an experimentally measured ultrasonic resonance spectrum of a freely vibrating crystal with well-defined shape (Fig. 5). The main advantages offered by RUS are (i) the elastic, piezoelectric and dielectric properties of the crystal can be in principle simultaneously studied on one sample, (ii) the small sample size, (iii) no medium is required for transducer-sample coupling and (iv) the very short data acquisition time. Detailed reviews of this very promising technique have been recently published [26]. The principles of RUS and its advantages and challenges (if not to say disadvantages) are briefly described in this section.

The natural vibrational modes of a sample correspond to stationary solutions of its Lagrangian

$$L = \int (E_{\text{kinetic}} - E_{\text{potential}})dV$$

Following Hamilton and using the Ritz prescription, *i.e.* expanding the displacement vector $\xi = \xi_i \mathbf{e}_i$ and the electric potential ϕ in sets of basis functions $\{f_m\}$, $\{g_m\}$ according to $\xi_i = a_{im} f_m$ and $\phi = b_m g_m$, respectively, one obtains stationary solutions by solving the general eigenvalue problem

$$(\mathbf{G} + \mathbf{K}\mathbf{E}^{-1}\mathbf{K}^t)\mathbf{a} = \rho\omega^2\mathbf{M}\mathbf{a} \qquad (1)$$
$$\mathbf{b} = \mathbf{E}^{-1}\mathbf{K}^t\mathbf{a}$$

where $\nu = \omega/2\pi$ are the corresponding resonance frequencies and ρ is the mass density of the sample. The coefficients of the matrices **G**, **K**, **E** and **M** depend on the shape and dimensions of the sample as well as on the coefficients of the electromechanical property tensors of the crystal:

$$G_{(km)(in)} = \sum_{i,j} c^E_{klij} \int \frac{\partial f_m}{\partial x_l} \frac{\partial f_n}{\partial x_j} dV,$$
$$K_{(km)n} = \sum_{i,l} e_{ikl} \int \frac{\partial g_n}{\partial x_i} \frac{\partial f_m}{\partial x_l} dV,$$
$$E_{mn} = \sum_{i,j} \epsilon^S_{ij} \int \frac{\partial g_m}{\partial x_i} \frac{\partial g_n}{\partial x_j} dV,$$
$$M_{(km)(in)} = \int f_m f_n \delta_{ik} dV.$$

δ_{ij} denotes the Kronecker symbol. To keep the computational effort within reasonable limits, the size of the matrices must be restricted by the use of a truncated set of appropriate basis functions. A suitable choice are powers of Cartesian coordinates $f_m = x_1^{p1} x_2^{p2} x_3^{p3}, m = (p_1, p_2, p_3)$, because these functions can be easily applied to samples with simple shape (spheres, ellipoids, rectangular parallelepipeds, rods, cones *etc.*). The truncation condition $T \geq p_1 + p_2 + p_3$ leads to $N = (T+1)(T+2)(T+3)/6$ independent basis functions for the approximation of the electric potential and of each component of the displacement vector. While in cubic crystals about 1000 basis functions give a good compromise between accuracy and computing time sets of about 4000 basis functions or more are required in the case of monoclinic or triclinic crystals in order to avoid significant truncation errors.

Unfortunately, no analytical solution exists for the inverse problem. Thus the sample parameters have to be evaluated by an iterative non-linear least-squares procedure that matches observed and calculated resonance frequencies by adjusting values for the independent parameters. The convergence of a refinement depends critically on the proper choice of the initial values. Statistical [27] and experimental [28] procedures were proposed for mode identification in samples with high symmetry from which the derivation of starting values c^0_{ij} is expected. However, the use of conventional techniques for the determination of appropriate c^0_{ij} values is still necessary for crystals with low symmetry.

The progress of the refinement procedure is further affected by a number of errors originating from mechanical load on the sample, misorientation of the sample, deviations from the ideal shape and crystal defects. In particular, two-dimensional defects such as twin boundaries and cracks can make the quantitative interpretation of a resonance spectrum impossible because the sample has to be considered as a system of two or more resonators of unknown shape and dimensions coupled by springs of unknown force constants. More homogeneously distributed defects with dimensions much smaller than the elastic wavelength usually do not restrict the application of RUS.

Different experimental set-ups suited for samples of about 100 μm up to several meters in size and covering the temperature range from about 4K to 1800K have been reported (see [26] and references therein). RUS-apparatus for routine measurements are already commercially available [29].

For crystals with piezoelectric effects larger than about 30% of d_{111} of α-quartz and moderate dielectric constants the piezoelectric contribution to eigenfrequencies, as included by the term $\mathbf{K}\mathbf{E}^{-1}\mathbf{K}^t$ in (1), can be forced to be considerably larger than the experimental error (the reproducibility of experimental resonance frequencies is usually ±0.1 KHz or better) by choosing an appropriate sample size. Due to the strong anisotropy of piezoelectric properties, fortunately, in most cases no starting value problem exists for the computation of piezoelectric constants from resonance frequencies [30]. Employing the following procedure

- Step 1: Prerequisites are the precise knowledge of dielectric constants and of proper starting values for the elastic constants.
- Step 2: Refinement of c_{ij} neglecting piezoelectric coupling effects.
- Step 3: Simultaneous refinement of elastic and piezoelectric constants using any set of initial e^0_{ijk} values.

and using elastic and dielectric constants listed in Landolt-Börnstein [31] we were able to derive piezoelectric stress constants from ultrasonic resonance spectra in excellent agreement with literature data (Table 2). Larger deviations of up to 30% from literature values are only ob-

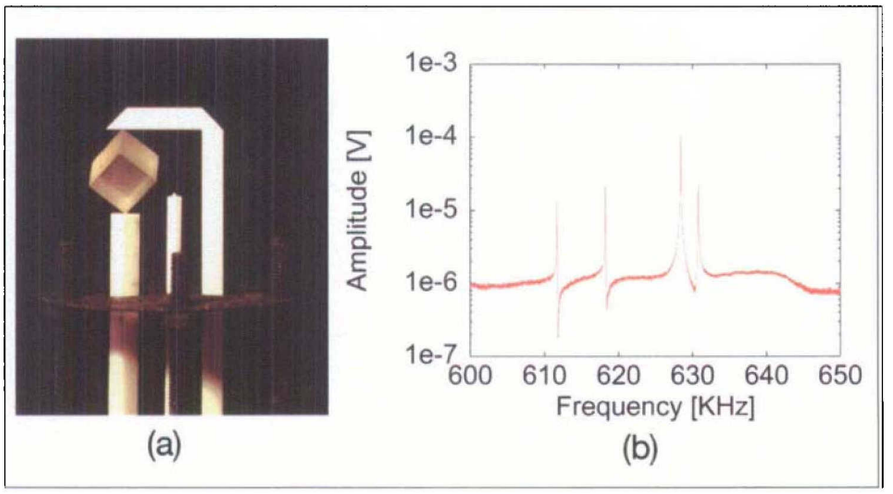

Fig. 5. (a) High-temperature RUS: A sample of monoclinic sanidine, $K_{0.89}Na_{0.11}AlSi_3O_8$, prepared as rectangular parallelepiped with edge lengths of about 5 mm is weakly clamped on two opposite corners by alumina buffer rods which act simultaneously as sample holder and as ultrasonic wave guides. Two piezoelectric transducers operating as ultrasonic generator and detector, respectively, are glued to the ends of the buffer rods outside the heated area. The central alumina tube supports a thermocouple. (b) Part of the resonance spectrum of a spodumene ($LiAlSi_2O_6$) sample showing four sharp eigenmodes. Note the logarithmic scale of the signal amplitude.

Table 2. Electromechanical coupling effects in selected piezoelectric crystals. Δf shift of resonance frequencies of the respective samples induced by electromechanical coupling; f_o, f_c observed and calculated resonance frequencies; $\Delta e_{ijk} = |(e_{ijk}^{LB} - e_{ijk})/e_{ijk}|$ relative difference between e_{ijk} calculated from resonance spectra and literature data e_{ijk}^{LB} taken from [31]. Resonance spectra have been collected on samples which are prepared as rectangular parallelepipeds with edge lengths in the range 4–9 mm.

Compound	PSG	Δf (maximum) [KHz]	$\lvert f_c - f_o \rvert$ (average) [KHz]	Δe_{ijk} (average) [%]	data/parameter ratio
$NaBrO_3$	23	0.2	0.28	0.5	12.5
$Cs_2S_2O_6$	6m	4.3	0.27	1.0	8.0
tourmaline (elbaite)	3m	1.0	0.24	2.8	8.1
$LiNbO_3$	3m	50.9	0.57	3.2	7.8
SiO_2 (α-quartz)	32	0.3	0.19	0.5	8.6
$La_3Ga_5SiO_{14}$	32	4.0	0.23	0.2	9.1
$Li_2SO_4 \cdot H_2O$	2	4.4	0.21	6.7	6.3

served for some of the small constants of monoclinic lithium sulfate monohydrate.

In summary, the RUS-technique is already a standard tool in non-destructive material testing. Other promising applications are the investigation of piezoelectric coupling phenomena, the study of the temperature dependence of elastic properties and the detection of phase transitions. The focus of current research is on the most challenging problem connected with the RUS-method: the derivation of proper initial values for the elastic constants from resonance spectra. Due to the ongoing rapid advances in computer technology the application of statistical and simulation methods will become feasible soon. An alternative approach is the estimation of starting values by lattice energy calculations [3].

Acknowledgement

I would like to acknowledge financial support from the Swiss National Science Foundation under grant No. 20-53630.98 and 2000-061482.00/1.

Received: April 18, 2001

[1] B. Winkler, *Z. Kristallogr.* **1999**, *214*, 506
[2] Berichte aus Arbeitskreisen der DGK, vol. 2, 'Predictability of physical properties of crystals', Ed. J. Schreuer, Kiel, **1998**. Berichte aus Arbeitskreisen der DGK, vol. 6, 'Measurement and interpretation of mechanical properties of crystals', Ed. J. Schreuer, Kiel, **2000**.
[3] B. Winkler, M. Hytha, M.C. Warren, V. Milman, J.D. Gale, J. Schreuer, *Z. Kristallogr.* **2001**, *216*, 67.
[4] Many authors use the term 'electrostriction' exclusively for the description of quadratic electromechanical effects. However, in this paper 'electrostriction' is used in a broader sense as the strain response of matter on an inducing electrical force. This includes the linear electrostriction or converse piezoelectric effect, respectively, and all higher order terms.
[5] J. Grindlay, H.C. Wong, *Canad. J. Phys.* **1969**, *47*, 1563.
[6] L. Bohatý, *Z. Kristallogr.* **1982**, *158*, 233; K. Uchino, L.E. Cross, *Ferroelectrics* **1980**, *27*, 35.
[7] S.W.P. van Sterkenburg, T. Kwaaitaal, W.M. van den Eijnden, *Rev. Sci. Instrum.* **1990**, *61*, 2318; S.W.P. van Sterkenburg, *J. Phys.* **1991**, *D24*, 1853.
[8] J. Schreuer, 'Kritische Untersuchungen zur Messung elektrostriktiver Effekte in Kristallen', Dissertation Universität Köln, **1994**; J. Schreuer, S. Haussühl, *J. Phys.* **1999**, *D32*, 1263.
[9] H. Burkard, W. Känzig, M. Rossinelli, *Helvetica Physica Acta* **1976**, *49*, 13; G. Balakrishnan, K. Srinivasan, R. Srinivasan, *J. Appl. Phys.* **1983**, *54*, 2875.
[10] R. Srinivasan, K. Srinivasan, *J. Phys. Chem. Solids* **1972**, *33*, 1079; R. Srinivasan, K. Srinivasan, *phys. stat. sol.* **1973**, *57*, 757; J. Shanker, T.S. Verma, A. Cox, J.L. Sangster, *Can. J. Phys.* **1981**, *59*, 1359; S.W.P. van Sterkenburg, T. Kwaaitaal, *J. Phys.* **1992**, *D25*, 843.
[11] M.A. Carpenter, E.K.H. Salje, *Eur. J. Mineral.* **1998**, *10*, 693.
[12] J.F. Nye, 'Physical properties of crystals', Oxford University Press, Oxford, **1957**.
[13] S. Haussühl, 'Kristallphysik', Verlag Chemie, Verlag Physik, Weinheim, **1983**.
[14] A.S. Nowick, 'Crystal properties via group theory', Cambridge University Press, Cambridge, **1995**.
[15] S. Haussühl, *Z. Kristallogr.* **1993**, *205*, 215.
[16] P. Hartman, W.G. Perdok, *Acta Crystallogr.* **1955**, *8*, 49; P. Hartman, W.G. Perdok, *Acta Crystallogr.* **1955**, *8*, 521; P. Hartman, W.G. Perdok, *Acta Crystallogr.* **1955**, *8*, 525.
[17] J. Schreuer, S. Haussühl, *Z. Kristallogr.* **1993**, *205*, 309; S. Haussühl, *Z. Kristallogr.* **1989**, *188*, 311.
[18] S. Haussühl, *Z. Kristallogr.* **1991**, *196*, 47.
[19] S. Haussühl, *Z. Kristallogr.* **1991**, *194*, 57.
[20] H. Küppers, H. Siegert, *Acta Cryst.* **1970**, *A26*, 401.
[21] S. Haussühl, *Phys. kondens. Materie* **1967**, *6*, 181.
[22] Handbook of elastic properties of solids, liquids, and gases, vol. I, 'Dynamic methods for measuring the elastic properties of solids', Eds. A.G. Every, W. Sachse, Academic Press, San Diego, **2001**.
[23] J.M. Brown, L.J. Slutsky, K.A. Nelson, L.T. Cheng, *J. Geophys. Res.* **1989**, *B94*, 9485; E.H. Abrahamson, J.M. Brown, L.J. Slutsky, J. Zaug, *J. Geophys. Res.* **1997**, *102*, 12253.
[24] H. Spetzler, A. Shen, G. Chen, G. Hermannsdorfer, H. Schulze, R. Weigel, *Phys. Earth Planet Int.* **1996**, *98*, 93; H.-J. Reichmann, R.J. Angle, H. Spetzler, W.A. Bassett, *Am. Mineral.* **1998**, *83*, 1357.
[25] J.P. Wolfe, 'Imaging phonons', Cambridge University Press, Cambridge, **1998**.
[26] R.G. Leisure, F.A. Willis, *J. Phys. Condens. Matter* **1997**, *9*, 6001; A. Migliori, J.L. Sarrao, 'Resonant Ultrasound Spectroscopy', Wiley Sons, New York, **1997**; J. Schreuer, *Z. Kristallogr.* **2001**, in preparation.
[27] H. Yasuda, M. Koiwa, *J. Phys. Chem. Solids* **1991**, *52*, 723.
[28] A. Stekel, J.L. Sarrao, T.M. Bell, Ming Lei, R.G. Leisure, W.M. Visscher, A. Migliori, *J. Acoust. Soc. Am.* **1992**, *92*, 663.
[29] DRS, Inc., 225 Lane 13, Powell, Wyoming, USA, *www.ndtest.com*.
[30] J. Schreuer, E. Haussühl, W. Steurer, *Z. Kristallogr. Suppl.* **1999**, *16*, 110; J. Schreuer, E. Haussühl, L. Bohaty, W. Steurer, *Z. Kristallogr. Suppl.* **2000**, *17*, 53.
[31] Landolt-Börnstein, vol. III/29b, 'Low frequency properties of dielectric crystals: Elastic constants', Ed. D.F. Nelson, Springer-Verlag, Berlin, Heidelberg, New York, **1992**; Landolt-Börnstein, vol. III/29a, 'Low frequency properties of dielectric crystals: Piezoelectric, pyroelectric and related constants', Ed. D.F. Nelson, Springer-Verlag, Berlin, Heidelberg, New York, **1993**.